

Novel Cyclopeptides for the Design of MMP Directed Delivery Devices: A Novel Smart Delivery Paradigm

El-Farouck Moustoifa · Mohamed-Anis Alouini · Arnaud Salaün · Thomas Berthelot · Aghleb Bartegi · Sandra Albenque-Rubio · Gérard Délérís

Received: 23 February 2010 / Accepted: 19 April 2010 / Published online: 8 May 2010
© Springer Science+Business Media, LLC 2010

ABSTRACT

Purpose Matrix metalloproteinases (MMP) are a family of proteolytic enzymes, the expression of which in a key step of tumor progression has been better defined recently. The studies highlighted the ongoing need for very specific inhibitors, substrates or release devices designed to be selective for one or at least very few MMPs.

Methods This report deals with the design, synthesis and *in vitro* evaluation of linear and especially novel cyclic peptidic moieties, embodying MMP cleavable sequences designed to answer these questions. FRET (fluorescence resonance energy transfer) labelling *via* chromophore-modified amino-acids was used to give access to enzyme kinetics.

Results Evaluation of these peptides showed that cyclisation gives rise to high specificity for certain MMP, suggesting that this approach could provide very specific MMP substrate. Moreover, cyclic structures present a very good plasma stability.

Conclusions These original derivatives could allow the design of MMP-controlled delivery devices, the specificity of which will be retained in complex biological media and *in vivo*.

KEY WORDS cancer · cyclic peptide · delivery device · fluorescent substrate · MMP

ABBREVIATIONS

ACN	acetonitrile
APMA	4-aminophenylmercuric acetate
DAC	7-diethylamino coumarin-3-carboxylic acid
DCM	methylene chloride
DIEA	N,N'-diisopropyl-diethylamine
DMF	N,N-dimethylformamide
DMSO	dimethylsulfoxide
EDC	1-ethyl-3-(3-dimethylaminopropyl) carbodiimide hydrochloride
ECM	extracellular matrix
Et ₂ O	diethyl ether
Fmoc	(9H-fluoren-9-ylmethoxycarbonyl)
FRET	fluorescence resonance energy transfer
HBTU	N-[1H-benzotriazol-1-yl]dimethylamino]methylene]-N-methylmethanaminium hexafluorophosphate N-oxide
HOBt	N-hydroxybenzotriazole
HPLC	high performance liquid chromatography
MALDI-TOF	matrix-assisted laser desorption/ionization—time of flight
MC	7-methoxy coumarin-3-carboxylic acid
MMP	Matrix metalloprotease
MMPI	MMP inhibitor
MS	mass spectrometry
NMM	N-methylmorpholine
PyBOP	benzotriazol-1-yl-oxy-tris-pyrrolidinophosphonium
tBu	t-butyl

E.-F. Moustoifa · M.-A. Alouini · A. Salaün · S. Albenque-Rubio · G. Délérís (✉)
Université Victor Segalen Bordeaux 2
CNRS UMR 5084 Bio-Organic Chemistry Group
146 rue Léo Saignat
F-33076 Bordeaux Cedex, France
e-mail: gerard.deleris@u-bordeaux2.fr

M.-A. Alouini · T. Berthelot
CEA, IRAMIS, LSI Irradiated Polymers Group
UMR 7642 CEA/CNRS/Ecole Polytechnique
F-91128 Palaiseau Cedex, France

M.-A. Alouini · A. Bartegi
Unité de Recherche 02/UR/09-01 Biochimie des Protéines et Interactions Moléculaires
Avenue Taher Hadda, BP 74, Monastir 5000, Tunisie

TFA	Trifluoroacetic acid
THF	tetrahydrofuran
TIS	triisopropylsilane
TRIS	tris(hydroxymethyl)aminomethane
Trt	trityl
SPPS	solid phase peptide synthesis

INTRODUCTION

Matrix Metalloproteinases (MMPs) are a family of Zinc metalloenzymes involved in the catabolism of extracellular matrix (ECM). The tissue remodelling occurs in normal physiological processes such as development and morphogenesis but also during the course of diseases such as arthritis, cardiovascular diseases and cancer. MMPs display a large set of ECM and non-ECM substrates. Such enzymes have long been associated with many types and stages of cancer and were thought to be essential but limited to basement-membrane penetration during tumor progression and metastasis (1–3). The relationship between specific MMP overexpression and tumor progression has been very recently highlighted (4,5). It has been shown that dramatic tumor escaping from antiangiogenic chemotherapies is correlated with MMP-2 and MMP-9 over-expression concomitant with MMP-1 downregulation. MMP monitoring could thus be envisaged as providing tools for diagnosis or prognosis. MMP expression profile can be considered as a tumor fingerprint. Matrix metalloproteinase are present globally in very low concentration, but concentrated on the surface of cells in tumor areas in high concentrated and activated form (6). For that reason, research for MMP inhibitors was very intensive about a decade ago. Several MMP-inhibitor (MMPI) drugs advanced up to phase III clinical trials in patients with advanced cancer, but the trials failed mainly because of muscle and joint pains which prevented reaching their end points of increased survival (7–10).

These results highlight the fact that previous MMPI development programs were initiated without adequate target validation and without identifying *in vivo* MMP substrates or their physiological roles. As previously pointed out, MMPs promote tumor progression not only through single ECM degradation, but also through a number of signaling functions (11–14). They are submitted to highly specific over-expression in dramatic phenomena linked to invasive phenotypic changes following anti-angiogenic therapies (4). The complexity of MMP over-expression and activities highlights their important role in metastatic diseases, especially in highly aggressive late-stage tumors with poor clinical outcome (15–18) and in dramatic situations when chemotherapy escaping occurs. Therefore,

the development of specific and selective substrate and/or inhibitors for one or a group of MMPs still remains of high interest for tumor targeting via mediation by MMP.

MMP activities have been previously addressed with synthetic fluorogenic derivatives both as biochemical and pharmacological tools, as well as for the design of targeted delivery systems. They are most often FRET-based substrates which were designed from natural collagen-identified sequences cleaved by MMPs while assuming additive thermodynamic contributions of different amino acids. Experimental conclusions highlight that this rationale is not fully convenient. To overcome this drawback, selectivity was addressed by G.B. Fields and coworkers with the synthesis of homotrimeric, fluorogenic triple-helical peptide (THP) models which include MMP cleavage sites (19).

Moreover, several delivery devices have also been designed, using polymeric vehicles (20,21), hydrogel matrix (22) or liposomal devices functionalized with peptidic moieties embodying MMP cleavage sequences. These previous studies confirmed that MMP-based release devices offer opportunities even if they present poor specificity (23,24). Moreover, as soon as peptidic structures are involved, requiring collagen-mimicking helicoidal entities, large numbers of amino-acids are included. Specific delivery at tumor areas upon MMP activation obviously remains a crucial challenge for the design of targeted anticancer therapies or imaging. It requires that reasonable size molecules, designed as MMP-cleavable devices, present a high level of selectivity for a very small number of selected MMP as well as high plasma stability.

One of the most frequently used approaches to improve peptide stability in biological medium is the cyclization of linear peptides, which prevents unspecific degradation by proteases. But direct cyclization of linear fluorogenic FRET-based peptides is not an acceptable approach, as the hydrolysis of sequence does not result in significant change of donor/acceptor proximity and thus does not allow enzymatic cleavage to be measured.

For these reasons, we herein propose a novel approach based on the design of cyclic peptides which incorporate two MMP substrate sequences. In order to test them, each fluorescent amino acid of a FRET probes pair was introduced between the substrate sequences. When hydrolyzed, the cyclic peptide releases fluorescent probes, and change in FRET signal provides access to cleavage kinetics. In order to validate the proof of concept for this approach, linear and cyclic MMP substrate peptides were synthesized and evaluated both *in vitro* and in plasmatic medium. We focused our attention on MMP-1 for its implication in metastatic process (15,25,26) and MMP-2 and MMP-9 for their over-expression in numerous steps of tumor progression (27).

MATERIALS AND METHODS

General Methods

All standard chemicals and solvents were of analytical grade and purchased from Sigma Aldrich. 2-Chloro chlorotriyl resin and all Fmoc-amino acids were purchased from Novabiochem.

Absorption spectra were recorded on a U-2010 Hitachi spectrophotometer (Hitachi instruments, USA). Enzymatic assays were recorded on a Luminescence Spectrometer model LS55 with a 4-position automatic cell changer including water thermostating and stirring for each sample position. Solid Phase Peptide Synthesis was carried out on an Applied Biosystems 433A automated peptide synthesizer. Reverse-phase HPLC was performed on a Hitachi LaChrom Elite equipped with an Organizer, Diode Array detector L-2450, Autosampler L-2200, pump L-2130 with a SATISFACTION RP18AB 5 μm 250 \times 4.6 mm C18 column for analytical session. Preparative HPLC was performed on a Shimadzu instrument equipped with a SCL-10 AVP system controller, LC8A HPLC pumps and SPD-10 AVP UV-vis detector probing at 214 nm on a SATISFACTION RP18AB 5 μm 250 \times 20 mm C18 column (C.L.I Cluzeau) for preparation. The following solvent systems were used for the elution in a linear gradient mode at a flow rate of 1 or 15 ml/min (for analytical and preparative HPLC respectively): (A) 0.1% aqueous trifluoroacetic acid (TFA) and (B) 0.1% TFA in 70% aqueous acetonitrile (ACN). MALDI-TOF mass spectrometry was performed on a BRUKER BIFLEX III mass spectrometer (CESAMO, Bordeaux, France) equipped with a nitrogen laser (337 nm, 3 ns pulse width).

Fluorescent Probes

Fluorescent amino acids, N^{ϵ} -(7-methoxycoumarin-3-carboxyl)-L-Fmoc lysine (i.e. Fmoc-Lys(MC)-OH) and N^{ϵ} -(7-diethylaminocoumarin-3-carboxyl)-L-Fmoc lysine (i.e. Fmoc-Lys(DAC)-OH) were synthesized as previously described by Berthelot *et al.* (28).

Peptide Synthesis (Table I)

Synthesis of **S1**, **S2** and **S9**

S1, **S2** and **S9** were synthesized using Fmoc strategy. A preloaded resin Fmoc-Ala-Wang Resin (0.72 mmol/g) was used for the synthesis (0.25 mmol; 350 mg). N^{α} -Fmoc amino acids (Gly, Leu, Pro, Gln(Trt), His(Trt), Tyr(tBu), Ala, Val, Lys(DAC), Lys(MC)) were used in a four-fold excess using HBTU in the presence of HOBt and DIEA. The synthesis was performed without capping, giving N -deprotected peptide-bound resin.

Peptides were cleaved from the resin by treatment with TFA/H₂O/TIS (95:2.5:2.5) mixture for 1 h 30 at room temperature. The resin was removed by filtration and washed with TFA (10 mL). The filtrate was evaporated under reduced pressure. The product was precipitated with cold diethyl ether. The crude peptides were collected by filtration and purified by preparative HPLC (C18) to yield **S1** (55 mg) MALDI-TOF m/e ($M+H^+$) 1484.64 (theoretical:1483.73 Da), **S2** (96 mg) MALDI-TOF m/e ($M+H^+$) 1541.56 (theoretical:1540.69 Da) and **S9** (102 mg) MALDI-TOF m/e ($M+H^+$) 1411.65 (theoretical:1410.68 Da).

Synthesis of **Sc1**, **Sc2** and **Sc9** by on Resin Cyclisation

Sc1, **Sc2** and **Sc9** were synthesized on a 0.2 mmol scale using Fmoc strategy. Fmoc-Glu-OAllyl (818 mg, 2 mmol) was dissolved in dry DCM (10 mL). After complete dissolution, DIEA (367 μL , 2.2 mmol) was added. After 10 min, 2-chloro chlorotriyl resin (1 g, 1.3 mmol/g) was added. The resulting suspension was stirred at room temperature for 5 h. The resin was filtered off and successively washed with DCM (3 \times 10 mL), DCM/methanol/DIEA (17/2/1) (4 \times 10 mL), DMF (2 \times 10 mL) and DCM (3 \times 10 mL). Resin was dried under high vacuum over KOH. 0.23 mmol/g substitution level was estimated by UV determination of the concentration of liberated dibenzofulvene after Fmoc group cleavage with piperidine. The Fmoc-Glu-OAllyl-trityl resin was packed in the reaction column of the automatic peptide synthesizer (437 mg, 0.1 mmol). N^{α} -Fmoc amino acids (Gly, Leu, Pro, Gln(Trt), Ala, Val, Lys(DAC), Lys(MC)) were used in a four-fold excess using HBTU in the presence of HOBt and DIEA. The synthesis was performed without capping, giving N -protected peptide-bound resin. This peptidyl resin was dried at 40°C under high vacuum for 4 h and then flushed with a stream of argon. Pd(PPh₃)₄ (693 mg, 0.6 mmol) was dissolved by bubbling a stream of Ar in a mixture of chloroform/acetic acid/*N*-methylmorpholine (8 mL, 37:2:1). Then, this mixture was transferred into reaction column containing the resin and was occasionally stirred with gentle agitation for 2 h at room temperature. Resin was filtered off and washed consecutively with 0.5% DIEA in DMF (3 \times 10 mL) and sodium diethyldithiocarbamate (0.5% w/w) in DMF (3 \times 10 mL) to remove the catalyst. Resin was successively washed with DMF (2 \times 10 mL) and DCM (3 \times 10 mL). After removal of Fmoc protecting group, resin was washed with 1 M HOBt in DMF. Peptidyl resin was mixed with a solution of PyBOP (260 mg, 0.5 mmol), HOBt (69 mg, 0.5 mmol) and DIEA (180 μL , 1 mmol) in *N*-methylpyrrolidone (10 mL). Mixture was swelled at room temperature for 48 h. Peptidyl resin was washed with DMF (2 \times 10 mL) and DCM (3 \times 10 mL). Peptides were cleaved from the resin by treatment with

Table 1 Structure of Linear (S1, S2, S9) and Cyclic (Sc1, Sc2, Sc9) Peptides

Peptide	Structure
S1	$H_2N\text{-Lys(DAC).Gly-Pro-Gln-Gly-Leu-Leu-Gly-Ala-Lys(MC)-Ala-COOH}$
S2	$H_2N\text{-Lys(DAC)-Pro-Pro-Gly-Ala-Tyr-His-Gly-Ala-Lys(MC)-Ala-COOH}$
S9	$H_2N\text{-Lys(DAC)-Gly-Pro-Gly-Gly-Val-Val-Gly-Pro-Lys(MC)-Ala-COOH}$
Sc1	$\text{Cyclo(Gly-Pro-Gln-Gly-Leu-Leu-Gly-Ala-Lys (DAC)-Gly-Pro-Gln-Gly-Leu-Leu-Gly-Ala-Lys(MC)-Glu)}$
Sc2	$\text{Cyclo(Pro-Pro-Gly-Ala-Tyr-His-Gly-Ala-Lys(DAC)-Pro-Pro-Gly-Ala-Tyr-His-Gly-Ala-Lys(MC)-Glu)}$
Sc9	$\text{Cyclo(Gly-Pro-Gly-Gly-Val-Val-Gly-Pro-Lys(DAC)-Gly-Pro-Gly-Gly-Val-Val-Gly-Pro-Lys(MC)-Glu)}$

TFA/H₂O/TIS (95:2.5:2.5) mixture for 1 h 30 at room temperature. Crude peptide was collected by filtration and purified by HPLC (C18). Preparative HPLC yielded **Sc1** (6 mg) MALDI-TOF m/e (M+Na⁺) 2240.13 (theoretical: 2217.11 Da) and **Sc9** (12 mg) MALDI-TOF m/e (M+H⁺) 2072.67 (theoretical: 2071.005 Da) .

Synthesis of **Sc1**, **Sc2** and **Sc9** by Cyclisation in Solution

Sc1, **Sc2** and **Sc9** were synthesized on a 0.25 mmol scale using Fmoc strategy. Fmoc-Glu(OtBu)-OH (850 mg, 2 mmol) was dissolved in dry DCM (10 mL). After complete dissolution, DIEA (367 μ L, 2.2 mmol) was added. After 10 min, 2-chloro chlorotriyl resin (1 g, 1.3 mmol/g) was added. The resulting suspension was stirred at room temperature for 5 h. The resin was filtered off and successively washed with DCM (3 \times 10 mL), DCM/methanol/DIEA (17/2/1) (4 \times 10 mL), DMF (2 \times 10 mL) and DCM (3 \times 10 mL). Resin was then dried under high vacuum over KOH. 0.76 mmol/g substitution level for this preloaded resin was estimated by UV determination of the concentration of liberated dibenzofulvene, after the cleavage of the Fmoc group with piperidine. Fmoc-Glu(OtBu)-trityl resin (329 mg) was packed into the reaction column of the automatic peptide synthesizer. *N*^α-Fmoc amino acids (Gly, Leu, Pro, Gln(Trt), His(Trt), Tyr(tBu), Ala, Val, Lys(DAC), Lys(MC)) were used in a four-fold excess using HBTU in the presence of HOBT and DIEA. Synthesis was performed without capping, giving *N*-deprotected peptide-bound resin. Repetitive treatment of peptidyl resin with a 0.6% TFA solution in dichloromethane (16 \times 10 mL) was carried out in a sealable sintered glass funnel (1 min per treatment). Resin was filtered into a flask containing 10% of pyridine in DCM (2 mL of pyridine in 20 mL of DCM). After evaporation under reduced pressure, 40 mL of water were added and the mixture cooled with ice to aid precipitation of the product. In the case of **Sc9**, the crude peptide was washed with 30 mL water without adding organic solvent. Resulting product was dried overnight.

In order to perform cyclization, crude peptide (0.25 mmol) was mixed with 500 mL DCM, EDC (1-ethyl-3-(3-dimethylaminopropyl) carbodiimide hydrochloride) (230 mg, 1.2 mmol) and HOBT (183.6 mg, 1.2 mmol) for 48 h. The final estimated concentration of peptide was close to 0.5 mM. After evaporation under reduced pressure to around 10 mL, 20 mL were added to wash the organic solution. After extraction and total evaporation of DCM, the sample was triturated and filtered with cold diethyl ether to reduce the presence of HOBT. Peptides were fully deprotected by treatment with TFA/H₂O/TIS (95:2.5:2.5) mixture for 1 h at room temperature. TFA was evaporated under reduced pressure, and the product was precipitated with cold diethyl ether. Crude peptide was collected by filtration and purified by preparative HPLC (C18) to yield **Sc1** (18 mg) MALDI-TOF m/e (M+Na⁺) 2240.13 (theoretical: 2217.11 Da), **Sc2** (135 mg) MALDI-TOF m/e (M+H⁺) 2332.00 (theoretical: 2331.038 Da) and **Sc9** (61 mg) MALDI-TOF m/e (M+H⁺) 2072.67 (theoretical: 2071.005 Da).

Fluorescence Spectra

All spectra were carried out in a total 2 mL volume. Slit width was 3.4 for emission and 12 for the excitation. Spectra were recorded in 0.1 M TRIS, 0.1 M NaCl, 10 mM CaCl₂, 0.05% of Igepal(CA-630), pH=7.4. Peptide concentrations were calculated using the molar extinction coefficient of MC and DAC in peptide: $\lambda_{360\text{nm}}$ (MC)= 18,500 M⁻¹cm⁻¹ and $\lambda_{436\text{nm}}$ (DAC)=26,300 M⁻¹cm⁻¹ for linear peptide. This coefficient is different in cyclic peptide, $\lambda_{360\text{nm}}$ (MC)=10,714 M⁻¹cm⁻¹ and $\lambda_{436\text{nm}}$ (DAC)= 19,291 M⁻¹cm⁻¹.

Enzyme Assays

MMP assays were performed in the same buffer described below. 20 μ L aliquot of 220 nM commercial MMP-1, MMP-2 and MMP-9 as zymogen form were activated with 10 μ M solution of 4-aminophenylmercuric acetate (APMA) (2 μ L, Buffer TRIS 0,1 M pH=9) at 37°C for 3 h. Stock

peptide solutions were prepared in DMSO (3 mg peptide in 200 μ L pure DMSO). For each measurement, peptide concentration was calculated using the molar extinction coefficient previously described. All assays were carried out in a total 2 mL volume with 2 nM activated MMP. After addition of enzyme to initiate reaction, the initial rate of substrate hydrolysis was determined by monitoring the increase in 401 nm fluorescence emission using a 350 nm excitation wavelength. Initial velocities were calculated in order to fit a Lineweaver-Burk plot for determination of kinetics parameter K_{cat} and K_m .

Plasma Assays

Blood was collected from voluntary donor at “Etablissement Français du Sang” (Bordeaux Site). Donors were tested and determined negative for HIV-1 and HIV-2, Hepatitis B and C HTLV-I/II viruses, and syphilis. Freshly collected plasma (immediately after control) containing 1.8 mg/ml EDTA 2 K (ethylene diamine tetraacetic acid dipotassium salt) were centrifuged 15 min at 1300 \times g. Plasma was then isolated. For every experiment, plasma tubes coming from three donors were pooled. All assays were carried out in a total 2 mL volume with 4 μ L of crude plasma and 4 μ M substrate added. The increase in fluorescence emission was monitored during 1 h at 401 nm using a 350 nm excitation wavelength. For the corresponding assays, activated MMP (1, 2 or 9) was subsequently added to the solution, and the fluorescence emission was monitored as described above again for 1 h.

RESULTS AND DISCUSSION

Novel FRET peptidic substrates were obtained by incorporation of fluorescent amino acids, N^{ϵ} -(7-methoxycoumarin-3-carboxyl)-L-Fmoc lysine (Fmoc-Lys(MC)-OH) as the donor and N^{ϵ} -(7-diethylaminocoumarin-3-carboxyl)-L-Fmoc lysine (Fmoc-Lys(DAC)-OH) as acceptor (28). These probes appear to be attractive due to their extended spectral range, high emission quantum yields, photostability, good solubility in the safest solvents and easy incorporation in a peptide sequence through solid phase peptide synthesis (SPPS) (29). These moieties previously allowed us

to monitor MMP activity (29). For that purpose, our substrates were designed from described sequences arising from Nagase *et al.* (30), which were described as MMP natural cleavage sites (Table II).

Peptide Synthesis

Fluorogenic amino acids were introduced as any other amino acid in the sequence, by solid phase synthesis, in order to provide the corresponding FRET peptide (Fig. 1). Linear fluorogenic substrates **S1**, **S2** and **S9** were obtained in satisfactory yields (Table III).

As tridimensional structural requirements are important for proteolytic activity and selectivity of MMPs, the design of conformationally restrained derivatives was an obvious target in our strategy. We herein report the first study involving conformationally restrained peptides after cyclization.

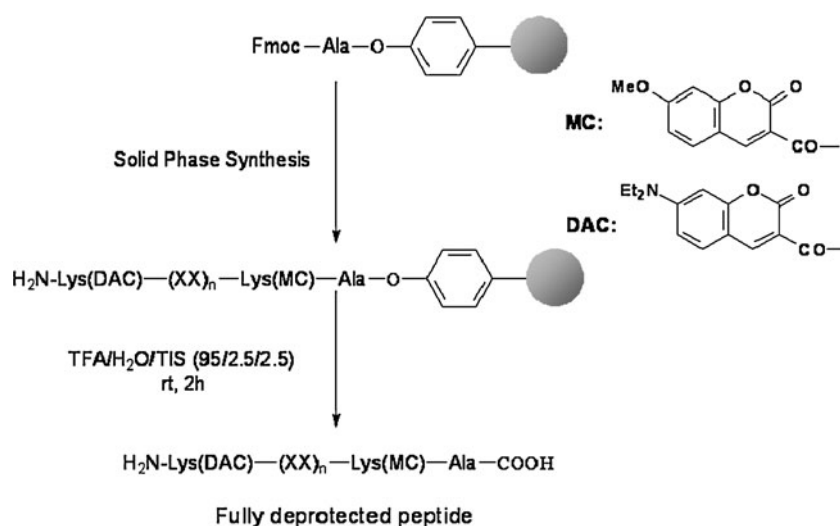
Cyclic moieties were first synthesized through a “head-to-tail” on resin cyclization. This synthetic approach is based upon the anchoring of the peptide to the resin through a side chain. Glutamic acid was used, protected with allyl group as an orthogonal α -carboxyl protection (34–36). Solid-phase synthesis of this cyclopeptide was performed on 2-chloro chlorotrityl resin. Loading of the resin was achieved to yield a low loaded resin (0.23 mmol/g) in order to improve intramolecular cyclization. Unfortunately, only cyclopeptides **Sc1**, **Sc9** were obtained in poor yields (Table IV) after a tricky HPLC purification step.

Because of the poor yields obtained from on-resin cyclisations, we prepared cyclic peptide through in-solution cyclisations. Fmoc-Glu(OtBu)-OH was loaded on a 2-chloro chlorotrityl resin. After automatic solid phase peptide synthesis, the fully protected peptide was removed from resin with diluted TFA (1%) on DCM. Cyclisation was then performed at 0.5 mM of peptide in presence of EDC and HOBt during 48 h in DCM (Fig. 2). No oligomeric fraction was observed in these conditions, and cyclic peptides were obtained with better yield after classical purification with water and acetonitrile/water (70/30) mixtures in presence of 0.1% TFA (Table IV). Even if peptide cyclization appeared to be more efficient in solution, cyclization step appeared here again to be strongly dependent on peptide sequence.

Table II Natural MMP Cleavage Sites

Sequence	Natural substrate	MMP	Ref
Gly-Pro-Gln-Gly ₇₇₅ -Leu ₇₇₆ -Leu-Gly-Ala	α_2 chain—Human collagen I	MMP-1, -8	(31)
Pro-Pro-Gly-Ala ₆₂ -Tyr ₆₃ -His-Gly-Ala	Human galectin-3	MMP-2	(32)
Gly-Pro-Gly-Gly ₄₃₉ -Val ₄₄₀ -Val-Gly-Pro	α_1 chain - Human collagen XI	MMP-9	(33)

Fig. 1 Synthesis of linear MMP-1, MMP-2 and MMP-9 substrates. Fmoc-Ala-Wang preloaded resin was used for synthesis.



Enzymatic Assays

Linear peptide embodying Lys (DAC) and Lys (MC) at N and C terminus revealed to be slightly hydrophobic. A stock solution of peptide in DMSO had yet to be achieved. Final concentration of DMSO (0.04–0.01% v/v) in the assay solution should not interfere with enzyme performance (37).

Peptides were treated with 2 nM of each activated enzyme (MMP-1, MMP-2 and MMP-9). Initial rates of hydrolysis were determined at various peptide concentrations. Data were used to construct Lineweaver-Burk plots in order to calculate k_{cat} and K_m (Fig. 3).

The second-order rate constant, k_{cat}/K_m , was determined for each enzyme and each substrate (Table V).

Surprisingly, **S1** from collagenase 1 natural substrate sequence exhibited a high affinity for gelatinases MMP2 and MMP-9. k_{cat}/K_m values were, respectively, $5.0 \cdot 10^6 \text{ M}^{-1} \cdot \text{s}^{-1}$ and $3.4 \cdot 10^6 \text{ M}^{-1} \cdot \text{s}^{-1}$ for MMP-2 and MMP-9. This represents a 20-fold increased ratio for MMP-2 and 14-fold for MMP-9 with regard to MMP-1 ($2.5 \cdot 10^5 \text{ M}^{-1} \cdot \text{s}^{-1}$). **S2** did not undergo significant cleavage when treated with MMP-1. As expected, **S2** is three times more recognized by MMP-2 with respective values $6.1 \cdot 10^5 \text{ M}^{-1} \cdot \text{s}^{-1}$ and $1.9 \cdot 10^5 \text{ M}^{-1} \cdot \text{s}^{-1}$ for MMP-2 and MMP-9. Similar

to **S2**, **S9** did not undergo significant cleavage when treated with MMP-1, while there is no significant difference between MMP-2 and MMP-9 (respectively, $6.2 \cdot 10^4 \text{ M}^{-1} \cdot \text{s}^{-1}$ and $3.8 \cdot 10^4 \text{ M}^{-1} \cdot \text{s}^{-1}$). Thus, **S2** and **S9** exhibited a very good selectivity for gelatinase family (MMP-2 and MMP-9), and **S2** offers a good specificity for MMP-2. The use of coumarin-modified amino acids seems to play a key role in the affinity of these peptides to the enzyme catalytic site.

When focusing on cyclic peptides, we could observe that **Sc1** cleavage properties *versus* MMP-1 were roughly unchanged compared with **S1** ($1.7 \cdot 10^5 \text{ M}^{-1} \cdot \text{s}^{-1}$). However, interestingly, MMP-2 and MMP-9 activities on this derivative were notably decreased with respect to k_{cat}/K_m $6.1 \cdot 10^5 \text{ M}^{-1} \cdot \text{s}^{-1}$ and $6.9 \cdot 10^5 \text{ M}^{-1} \cdot \text{s}^{-1}$.

While almost no selectivity could be observed between the three MMP towards **Sc9**, cyclic peptide **Sc2** was only recognized by MMP-9.

Indeed, no significant cleavage was observed either with MMP-1 or MMP-2, while k_{cat}/K_m ($9.3 \cdot 10^5 \text{ M}^{-1} \cdot \text{s}^{-1}$) is only two times less than the value of linear form *versus* this enzyme.

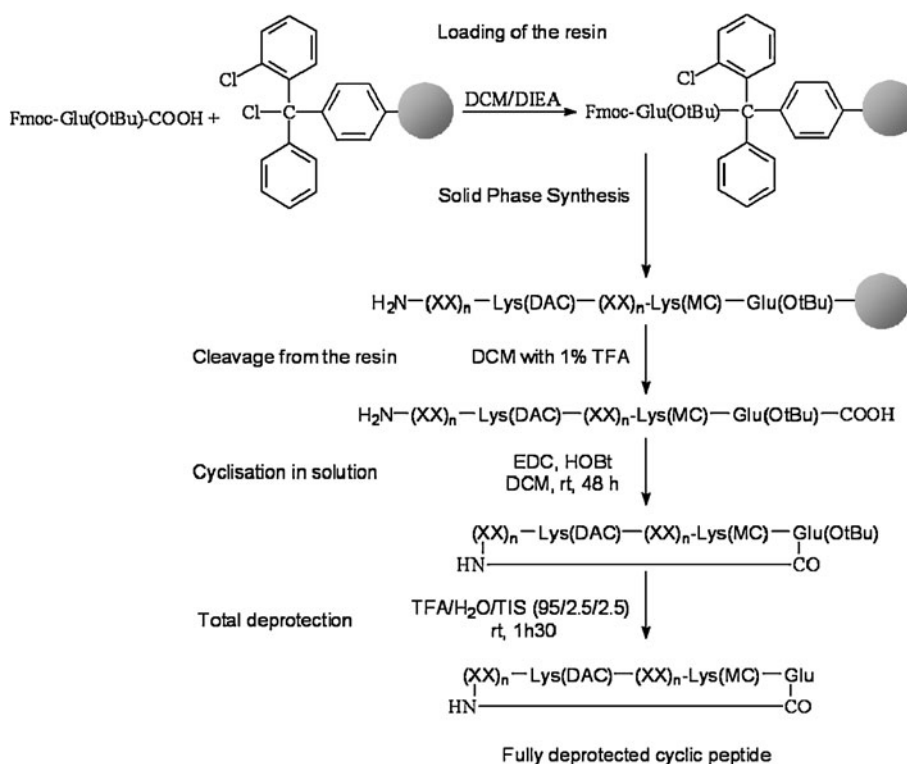
Table III Sequences of Novel Substrates

Compounds	Sequences	Yields
S1	$\text{H}_2\text{N-K(DAC)GPQG-LLGAK(MC)A-COOH}$	27%
S2	$\text{H}_2\text{N-K(DAC)PPGA-YHGAK(MC)A-COOH}$	46%
S9	$\text{H}_2\text{N-K(DAC)GPGG-WGPK(MC)A-COOH}$	42%

Table IV Cyclic Substrates Yields from On-Resin (A) and In-Solution (B) Cyclisations

Compound	Sequence	Yield %	
		A	B
Sc1	Cyclo[GPQGLLGAK(DAC)GPQGLLGAK(MC)E]	2.6	3.5
Sc2	Cyclo[PPGAYHGAK(DAC)PPGAYHGAK(MC)E]	–	23
Sc9	Cyclo[GPGGWGPK(DAC)GPGGWGPK(MC)E]	5.8	11

Fig. 2 Cyclopeptides synthesis via in solution cyclization. 2-chloro chlorotrityl resin was used for synthesis.



These results highlight that reasonably sized novel modified structures can reach a very high level of selectivity towards one specific MMP.

Plasma Stability

The use of our substrate in a drug delivery system implies a relatively good stability in biological sample in order to avoid non-specific release.

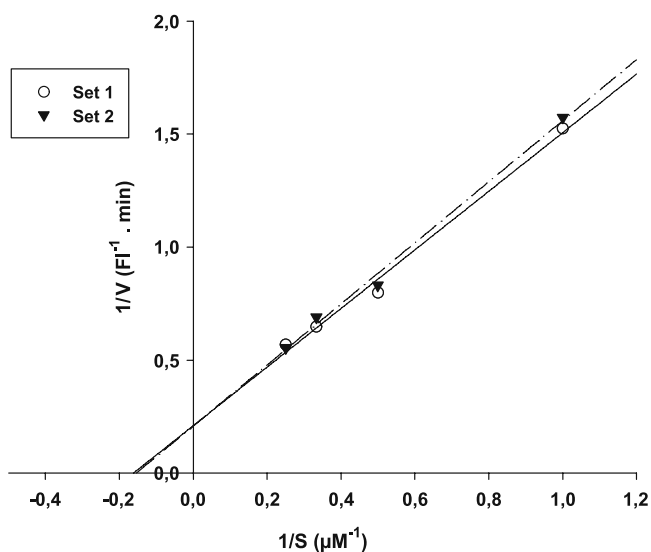


Fig. 3 Lineweaver-Burk analysis of **S1** hydrolysis by activated MMP-1 (2 nM). Fluorometric assay monitoring at 37°C, and substrate concentration range 1-4 μM.

Table V Kinetic Parameters of Enzyme (N.S.C: No Significant Cleavage)

Substrate	k_{cat} (s^{-1})	K_m (μM)	k_{cat}/K_m ($M^{-1} \cdot s^{-1}$)
MMP-1			
S1	1.57	6.3	$2.5 \cdot 10^5$
S2	N.S.C	N.S.C	N.S.C
S9	N.S.C	N.S.C	N.S.C
Sc1	1.09	6.3	$1.7 \cdot 10^5$
Sc2	N.S.C	N.S.C	N.S.C
Sc9	0.28	5.4	$5.2 \cdot 10^4$
MMP-2			
S1	15.8	3.1	$5.0 \cdot 10^6$
S2	2.84	4.6	$6.1 \cdot 10^5$
S9	0.29	4.7	$6.2 \cdot 10^4$
Sc1	2.19	3.39	$6.5 \cdot 10^5$
Sc2	N.S.C	N.S.C	N.S.C
Sc9	0.18	3.1	$5.6 \cdot 10^4$
MMP-9			
S1	17.6	5.1	$3.4 \cdot 10^6$
S2	0.96	4.9	$1.9 \cdot 10^5$
S9	0.43	11.3	$3.8 \cdot 10^4$
Sc1	5.11	7.4	$6.9 \cdot 10^5$
Sc2	0.95	10.2	$9.3 \cdot 10^4$
Sc9	0.33	6.8	$4.9 \cdot 10^4$

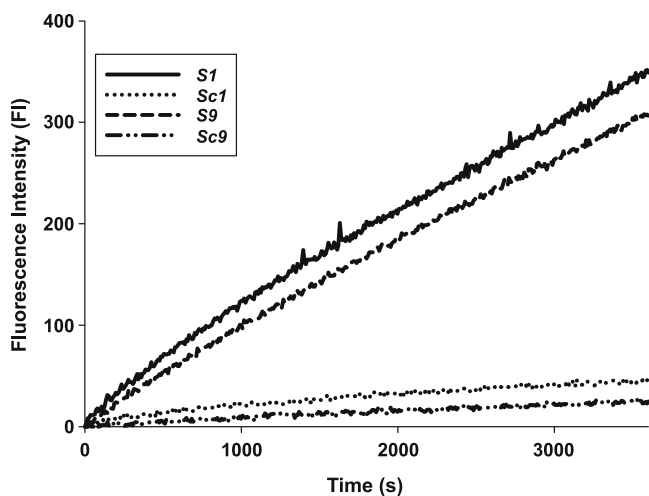


Fig. 4 Substrates digestion in plasma. Peptides were treated for 1 h with 4 μ l crude plasma.

In order to evaluate the stability, substrates were treated with plasma for 1 h (Fig. 4).

While linear compounds underwent rapid cleavage from aspecific plasma proteases, cleavage kinetics for **Sc1** and **Sc9**, respectively, decreased by a 10 and 13 factor. **Sc2** did not significantly cleave during the time of assays.

Addition of activated MMP-9 (1nM) into the previous assays led to a dramatic increase in cyclic peptide hydrolysis (Fig. 5). Results correlate with the ones obtained with pure enzymes, i.e. **Sc1** is more sensitive than **Sc2** or **Sc9** to the presence of activated MMP-9.

Results presented in Fig. 6 clearly demonstrated that, while linear **S2** is immediately proteolyzed within plasma, MMP addition highlights a very specific cleavage of **Sc2** by only one MMP, MMP-9 here.

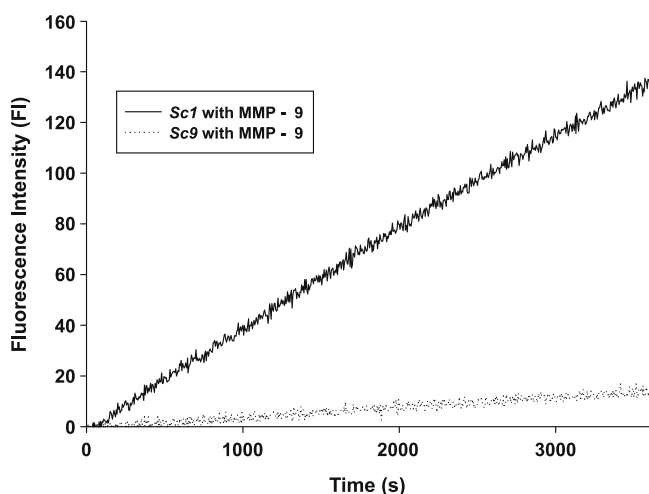


Fig. 5 Addition of 1nM activated MMP-9 to assay described Fig. 5. After 1 h digestion with plasma, activated MMP-9 was added to **Sc1** and **Sc9** plasmatic assay.

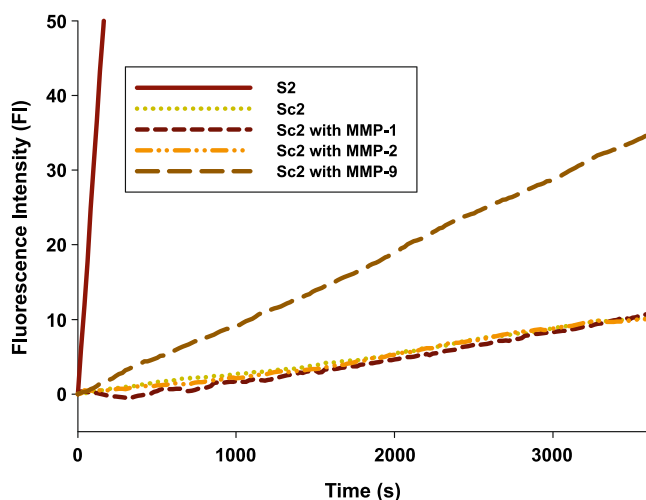


Fig. 6 Stability of **S2** and **Sc2** in plasma and subsequent treatment with MMP-1, MMP-2 or MMP-9. After 1 h plasma digestion, activated MMP-1, MMP-2 or MMP-9 was added to **Sc2** assay.

When activated MMP-1 or MMP-2 were added to the mixture, peptide cleavage remained very limited. On the contrary, hydrolysis of this specific substrate increased substantially upon addition of activated MMP-9.

CONCLUSION

Proposed design of original chemical moieties highlights a novel paradigm for specific delivery at tumor areas. Original reasonably sized cyclo-peptidic derivatives proved to be specifically cleaved by only one or at least selectively by one MMP. It has been proved that selective MMP over-expression is correlated with crucial stages or tumor progression. Therefore, these derivatives could behave as smart delivery devices at the zone of MMP expression under MMP activity itself, due to their plasma stability. Our results show that other proteolytic enzymes could be targeted after optimization.

Design of delivery devices will involve either covalent binding through glutamic acid side chain or via supramolecular design. Indeed, we have data (not published) proving that coumarine aromatic part may play an essential role in device stabilization through host guest interactions.

ACKNOWLEDGMENTS

Authors wish to warmly thank Dr. Pierre Voisin and Dr. Philippe Mellet for helpful discussions, Collectivité Départementale de Mayotte, Conseil Régional d'Aquitaine and Ligue Contre le Cancer for financial support.

REFERENCES

- Liotta LA. Metastatic potential correlates with enzymatic degradation of basement membrane collagen. *Nature*. 1980;284:67–8.
- Stetler-Stevenson WG. Progelatinase A activation during tumor cell invasion. *Invasion Metastasis*. 1994;14:259–68.
- Nagascand H, Woessner JF. Matrix metalloproteinases. *J Biol Chem*. 1999;274:21491–4.
- Lucio-Eterovic AK, Piao Y, de Groot JF. Mediators of glioblastoma resistance and invasion during antivasular endothelial growth factor therapy. *Clin Cancer Res*. 2009;15:4589–99.
- Roy R, Louis G, Loughlin KR, Wiederschain D, Kilroy SM, Lamb CC *et al*. Tumor-specific urinary matrix metalloproteinase fingerprinting: identification of high molecular weight urinary matrix metalloproteinase species. *Clin Cancer Res*. 2008;14:6610–7.
- Brooks PC, Stromblad S, Sanders LC, von Schalscha TL, Aimes RT, Stetler-Stevenson WG *et al*. Localization of matrix metalloproteinase MMP-2 to the surface of invasive cells by interaction with integrin alpha v beta 3. *Cell*. 1996;85:683–93.
- Zucker S, Cao J, Chen WT. Critical appraisal of the use of matrix metalloproteinase inhibitors in cancer treatment. *Oncogene*. 2000;19:6642–50.
- Coussens LM, Fingleton B, Matrisian LM. Matrix metalloproteinase inhibitors and cancer: trials and tribulations. *Science (New York, NY)*. 2002;295:2387–92.
- Overall CM. Molecular determinants of metalloproteinase substrate specificity: matrix metalloproteinase substrate binding domains, modules, and exosites. *Mol Biotechnol*. 2002;22:51–86.
- Fingleton B. Matrix metalloproteinase inhibitors for cancer therapy: the current situation and future prospects. *Expert Opin Ther Targets*. 2003;7:385–97.
- McCawley IJ, Matrisian LM. Matrix metalloproteinases: they're not just for matrix anymore! *Curr Opin Cell Biol*. 2001;13:534–40.
- Aoki T, Sumii T, Mori T, Wang X, Lo EH. Blood-brain barrier disruption and matrix metalloproteinase-9 expression during reperfusion injury: mechanical *versus* embolic focal ischemia in spontaneously hypertensive rats. *Stroke*. 2002;33:2711–7.
- Overall CM. Dilating the degradome: matrix metalloproteinase-2 cuts to the heart of the matter. *Biochem J*. 2004;383:E5–7.
- Parks WC, Wilson CL, Lopez-Boado YS. Matrix metalloproteinases as modulators of inflammation and innate immunity. *Nature Rev Immunol*. 2004;4:617–29.
- Minn AJ. Genes that mediate breast cancer metastasis to lung. *Nature*. 2005;436:518–24.
- Minn AJ, Kang Y, Serganova I, Gupta GP, Giri DD, Doubrovin M *et al*. Distinct organ-specific metastatic potential of individual breast cancer cells and primary tumors. *J Clin Invest*. 2005;115:44–55.
- Radisky DC, Levy DD, Littlepage LE, Liu H, Nelson CM, Fata JE *et al*. Rac1b and reactive oxygen species mediate MMP-3-induced EMT and genomic instability. *Nature*. 2005;436:123–7.
- Weigelt B, Peterse JL, van 't Veer LJ. Breast cancer metastasis: markers and models. *Nat Rev Cancer*. 2005;5:591–602.
- Lauer-Fields JL, Broder T, Sritharan T, Chung L, Nagase H, Fields GB. Kinetic analysis of matrix metalloproteinase activity using fluorogenic triple-helical substrates. *Biochemistry*. 2001;40:5795–803.
- Vartak DG, Gemeinhart RA. Matrix metalloproteinases: underutilized targets for drug delivery. *J Drug Target*. 2007;15:1–20.
- Chau Y, Tan FE, Langer R. Synthesis and characterization of dextran-peptide-methotrexate conjugates for tumor targeting via mediation by matrix metalloproteinase II and matrix metalloproteinase IX. *Bioconjug Chem*. 2004;15:931–41.
- Tauro JR, Lee BS, Lateef SS, Gemeinhart RA. Matrix metalloproteinase selective peptide substrates cleavage within hydrogel matrices for cancer chemotherapy activation. *Peptides*. 2008;29:1965–73.
- Tauro JR, Gemeinhart RA. Matrix metalloproteinase triggered delivery of cancer chemotherapeutics from hydrogel matrices. *Bioconjug Chem*. 2005;16:1133–9.
- Tauro JR, Gemeinhart RA. Extracellular protease activation of chemotherapeutics from hydrogel matrices: a new paradigm for local chemotherapy. *Mol Pharm*. 2005;2:435–8.
- Murray GI, Duncan ME, O'Neil P, Melvin WT, Fothergill JE. Matrix metalloproteinase-1 is associated with poor prognosis in colorectal cancer. *Nature Med*. 1996;2:461–2.
- Overall CM, Kleinfeld O. Validating matrix metalloproteinases as drug targets and anti-targets for cancer therapy. *Nat Rev Cancer*. 2006;6:227–39.
- Folgueras AR, Pendas AM, Sanchez LM, Lopez-Otin C. Matrix metalloproteinases in cancer: from new functions to improved inhibition strategies. *Int J Dev Biol*. 2004;48:411–24.
- Berthelot T, Lain G, Latxague L, Deleris G. Synthesis of novel fluorogenic L-Fmoc lysine derivatives as potential tools for imaging cells. *J Fluoresc*. 2004;14:671–5.
- Berthelot T, Talbot JC, Lain G, Deleris G, Latxague L. Synthesis of N epsilon-(7-diethylaminocoumarin-3-carboxyl)- and N epsilon-(7-methoxycoumarin-3-carboxyl)-L-Fmoc lysine as tools for protease cleavage detection by fluorescence. *J Pept Sci*. 2005;11:153–60.
- Nagase H, Gregg BF. Human matrix metalloproteinase specificity studies using collagen sequence-based synthetic peptides. *Pept Sci*. 1996;40:399–416.
- Fields GB. A model for interstitial collagen catabolism by mammalian collagenases. *J Theor Biol*. 1991;153:585–602.
- Ochieng J, Fridman R, Nangia-Makker P, Kleiner DE, Liotta LA, Stetler-Stevenson WG *et al*. Galectin-3 Is a Novel Substrate for Human Matrix Metalloproteinases-2 and-9. *Biochemistry*. 2002;33:14109–14.
- Niyibizi C, Chan R, Wu JJ, Eyre D. A 92 kDa gelatinase (MMP-9) cleavage site in native type V collagen. *Biochem Biophys Res Commun*. 1994;202:328–33.
- Flouzat C, Marguerite F, Croizet F, Percebois M, Monteil A, Combourieu M. Solid-phase synthesis of "head-to-side chain" cyclic tripeptides using allyl deprotection. *Tetrahedron Lett*. 1997;38:1191–4.
- Planas M, Bardaji E, Barany G. Synthesis of cyclic peptide hybrids with amino acid and nucleobase side-chains. *Tetrahedron Lett*. 2000;41:4097–100.
- Napolitano A, Bruno I, Rovero P, Lucas R, Peris MP, Gomez-Paloma L *et al*. Synthesis, structural aspects and bioactivity of the marine cyclopeptide hymenamamide C. *Tetrahedron*. 2001;57:6249–55.
- Gogly B, Groult N, Hornebeck W, Godeau G, Pellat B. Collagen Zymography as a Sensitive and Specific Technique for the Determination of Subpicogram Levels of Interstitial Collagenase. *Anal Biochem*. 1998;255:211–6.